Chapter 20

The ocean and climate change

In this final chapter we turn from the short-term climate variability of ENSO to consider variations with timescales of several decades or more. Small but persistent changes in climate can have a huge impact on the ecosphere (the finely tuned interplay between living matter and its environment). Such changes can occur naturally, as they have done in the past, experienced for example as ice ages and interglacial periods. This century is witnessing the possibility of climate changes through human activity. The last few decades have seen the introduction of the so-called greenhouse gases (CO_2, CH_4 and others) into the atmosphere on an ever increasing scale; this alters the radiation balance and may result in climate changes of magnitudes comparable to those which occurred naturally in the past. Many countries therefore have made research into these longer-term variations a national priority, and oceanographers are asked to quantify the role of the oceans in long-term climate change. However, when oceanographers try to come to grips with longer-term changes in the ocean, they immediately find themselves facing a major problem - the very patchy nature of the observational record. There have been large fluctuations in the number and spatial distribution of observations made over the decades, as shipping routes changed and wars interrupted continuous data collection and research plans. In many cases the technology used changed drastically over time, and data in the same series are not directly comparable. There is considerable risk that changes in observation density and technique may introduce bias, and great care has to be taken in interpreting long time series of ocean data. Nevertheless, as we shall see, there are several incontrovertible examples of changes in the ocean over decades, and some of these lend themselves to preliminary interpretation in terms of large-scale changes in the ocean circulation patterns.

Given the problems with the data, and the rapidly increasing sophistication of ocean numerical models, it is not surprising that climatologists have recently come to rely rather heavily on numerical models to explore the ways in which changes in ocean circulation are likely to occur. These models, and in particular those which couple the ocean with the atmosphere, have generated some valuable ideas about the likely nature of some kinds of longer-term climate variations. Some of these new ideas and their implications are discussed in this chapter.

Using models to extend our limited observational data base into the future is of course risky business, since few of the model predictions can be verified with existing data. Modellers and observationalists are both well aware of the dangers of predicting long-term climate variations in this way. One of the major goals of the international climate research community is therefore directed towards building an observing network that will keep track of climate changes throughout the world ocean, as well as in the atmosphere. How this can be achieved and what is on the drawing board is discussed at the end of this chapter.

The observations

Three major sources are available for inferring changes in ocean circulation over the last hundred years or so. The first is the record of sea surface temperature from merchant ships. Some 150 years ago Captain Matthew Fontaine Maury of the U.S. Navy introduced an

international program of data collection at sea, which has been gaining impetus ever since. Ship's officers have always recognized the value of good marine weather data (which was even more important in the days of sailing ships than today), and so the quality of the merchant ship record (though by no means perfect, as we shall see) is remarkably good. The extremely laborious task of entering all these decades of data from around the world into computer-compatible form is also now largely complete (there were about 63 million SST observations alone, to 1979); various versions of the world record of marine observations, known as the Comprehensive Ocean-Atmosphere Data Set or COADS, are now readily available for interested users, in various stages of editing and compression. In addition to sea surface temperature, this data set contains surface winds, air pressure, temperature and humidity, cloud cover and rainfall, which also provide valuable information from which - given our present understanding of the ocean as a dynamical system - changes in ocean circulation can be inferred. However, most of their value is in meteorology, and detailed discussion is beyond the scope of this book.

The second data set consists of a few long-term tide-gauge records, mostly from Europe and North America. These have been much studied in connection with the possibility of long-term sea-level rise as a result of increasing CO_2 levels. We will address both their limitations and the things that have been learned from them.

Thirdly, accurate profiles of ocean temperature and salinity throughout depth have been undertaken since the introduction of the Nansen bottle and the reversing thermometer, the precursors of the modern CTD, some 110 years ago. However, reliable sections across ocean basins do not go back further than about 70 years, and examples of high-quality sections that have been repeated a few decades apart are quite rare; thus the interpretation problem in this case is usually one of the representativeness of the data rather than one of data quality.

Sea surface temperature

In the early days of the merchant ship measurement program, sea surface temperature (SST) was measured by picking up a water sample in a canvas bucket and measuring its temperature when it reached the ship's deck. Evaporation from the bucket's walls will generally result in cooling, depending on weather conditions and the time taken to make the measurement. By contrast, for the last forty years SST has mostly been measured by devices installed in the intake for the engine cooling system; in this case water is usually warmed during its transit from the ocean to the thermometer. The difference between uninsulated bucket temperatures and engine room intake temperatures is generally in the range 0.3-0.7°C. Since the data forms filled out by the officers usually did not include a space for recording the device used for measurement (uninsulated bucket, insulated bucket or engine room thermograph), there is an inherent uncertainty in the long-term SST records. Reasonable assumptions have been made about the change of instrumentation through time, but these cannot now be directly checked. Similarly, air temperatures are often measured in rather sheltered locations that may be subject to deck heating during daytime, and such details are not recorded. Nevertheless, it has been found that when reasonable correction procedures are applied to each data set, the magnitude of the corrections turns out to be extremely consistent between, for example, the northern and southern hemisphere, and

the variations in corrected air and sea temperature track one another quite closely. This gives one some confidence that along major shipping routes averages of each time series over a 10°x10° square for a decade will be reliable to one or two tenths of a °C.

When processed in such a way, i.e. compressed into mean annual values for 10°x10° squares, sea surface temperature is seen to be a function f of space and time defined at constant space and time intervals: SST = f(x,y,t), where x, y represent the longitude and latitude of the centre of the 10°x10° square and t is the year. Several mathematical techniques are available to analyze space and time trends in such data sets. One method regularly used in meteorology and oceanography is a technique known as Empirical Orthogonal Function (EOF) analysis. The method represents the data as a sum of products of functions: f(x,y,t) = Σ F_i(x,y)G_i(t), where the F_i express the data distribution in space and the G_i give the contribution of the respective space distribution to the observed SST field at any given time. Theory shows that an infinite sum of function products can reproduce the observations to any required accuracy and that many such representations of the data are possible. In practical applications the summation is truncated after the first few terms. The strength of EOF analysis lies in the fact that it arranges the contributions of the sum in such a way that the first term ($i = 1$) accounts for more of the variance found in the observations than any other term; the second term ($i = 2$) then accounts for more of the variance found in the difference between the observations and the first term than any of the following terms, and so on. This allows one to extract the dominant spatial and temporal signals with the help of very few function products.

Figures 20.1 - 20.3 show results of an EOF analysis of SST based on a data set similar to COADS but going back to "only" 1900. F_1(x,y), the space function for the first EOF, is shown in Figure 20.1a, while Figure 20.1b shows the corresponding time function G_1(t). The space function is seen to be positive nearly everywhere, and the time function is increasing irregularly with time. The net increase in G_1(t) over the last 80 years is about 0.5°C. The net contribution of the first EOF to SST is given by the product of both functions, which is negative everywhere before 1940 and turns positive from 1975 or so.

This provides fairly convincing evidence that - despite the uncertainties discussed earlier - the sea surface temperature has indeed risen over the present century by about 0.5°C on global average. However, it should be noted that this interpretation relies in part on the particular presentation of the first EOF; a similar analysis for the COADS data set which goes back another fifty years shows the same trend but cooling between 1860 and 1910 (Folland *et al.*, 1984).

As outlined above, the first EOF can be subtracted from SST(x,y,t) and the same analysis applied to the resulting difference, to give the second EOF which describes most of the remaining SST variation. The spatial pattern F_2(x,y) is seen in Figure 20.2a and the corresponding time amplitude G_2(t) in Figure 20.2b. In this case the spatial pattern has a maximum in the eastern Pacific Ocean and is in general closely reminiscent of the ENSO pattern of SST variability seen in Figure 19.6. Furthermore, the time amplitude G_2(t) has maxima at each of the ENSO events. It follows that during ENSO years the product F_2(x,y)G_2(t) has positive values (positive SST anomalies) in the eastern Pacific and negative values (negative SST anomalies) in the western Pacific Ocean, while the reverse is true during anti-ENSO years. In other words, the second EOF can be identified with the ENSO signal in SST discussed in Chapter 19. (EOF analysis also reveals that ENSO events are associated with a *global* warming of the ocean surface; this is seen in the first EOF which shows maxima in G_1(t) during ENSO years.)
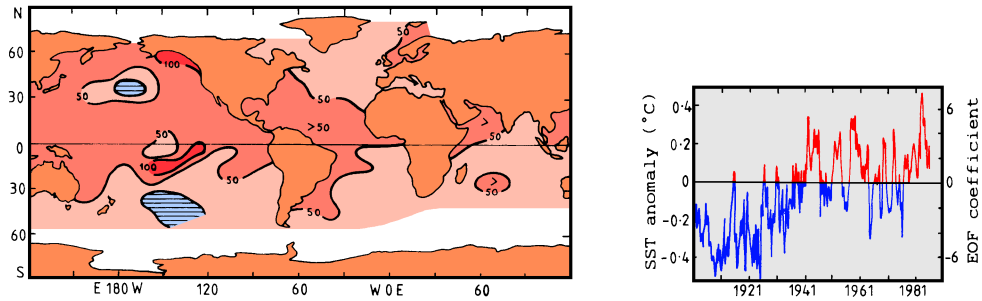
Fig. 20.1. Empirical Orthogonal Eigenfunction analysis of sea surface temperature. First eigenfunction: (a) spatial pattern (arbitrary units, negative values hatched), (b) temporal amplitude. From Folland *et al*. (1986a)
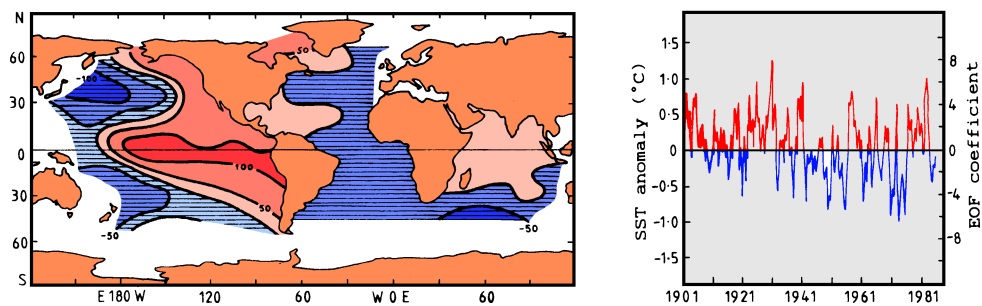

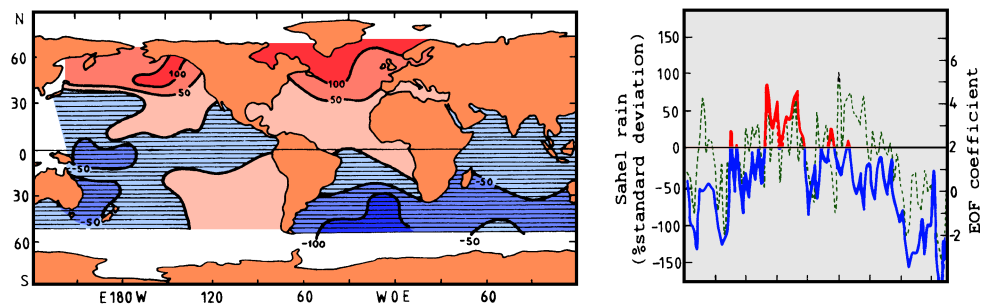Fig. 20.2. As for Fig. 20.1 but for the second Empirical Orthogonal Eigenfunction.

Fig. 20.3. As for Fig. 20.1 but for the third Empirical Orthogonal Eigenfunction. The dashed line in Fig. 20.3b shows an area average of rainfall in the Sahel region.

Subtracting the second EOF and applying the procedure once again produces the third EOF shown in Figure 20.3. $F3$(x,y) shows positive values in the north Atlantic and north Pacific Oceans and negative values through most of the Southern Hemisphere, while the time function shows slow variation over several decades. It might be thought that after such mathematical manipulations the result would be more noise than signal; however, there is

such strong spatial and temporal coherence in F_3 and G_3 that this is unlikely. Furthermore, both functions seem to be associated with significant changes in the world's climate. An idea of the magnitude of these effects can be gained from the fact that between 1950 and 1980, the temperature of the southern hemisphere oceans (plus the northern Indian Ocean) increased relative to the rest of the northern hemisphere oceans by about 0.4°C.

Figure 20.3b includes a measure of average rainfall in the Sahel region at the southern edge of the Sahara Desert. There is evidently a fair degree of correlation between the rainfall time series and the third EOF time function G_3(t) of SST. To test whether this correlation is a coincidence or is based in physics, atmospheric numerical models have been run with the SST anomalies of Figure 20.3a superimposed on a mean SST climatology. These generate rainfall anomalies over tropical Africa fairly similar to observation. A plausible explanation is that addition of the SST pattern of Figure 20.3a to climatology shifts the tropical SST maximum northwards. As discussed in the previous two chapters, this tends to move the rainfall maximum north with it. However, the true explanation may be more complex than this, and some time will pass before climatologists will be able to assist the people of the Sahel region to avoid the hardship and suffering which they experience during the present series of droughts.

These examples show that observed changes in SST can be related to observed variations in climate. It is therefore realistic to hope that with our increasing data base we will be able one day to go beyond mere description and come to conclusions about causes and effects.

Sea level measurements and sea level rise

Unlike the merchant ship data for which results are usually averaged over observations from a large number of ships, each tide gauge is an individual instrument. Its reliability over decades depends on the care taken by its operators in preventing fouling and damage, in meticulously recording any shifts in the tide staff fixed to a wall next to the gauge, and in taking accurate surveys every few years to relate the height of the staff to stable bench marks on the shore. 179 stations exist with records of more than 30 years; only 22 of these have records of more than 80 years, and of these only 3 are located outside the northeast Atlantic Ocean. Figure 20.4 shows the locations of sites with records of more than 10 years.

Many of these 179 records have to be rejected for use in long-term climate studies. For example, much of the coast of Japan and western North America is tectonically active, so that all the bench marks to which the tide gauge height has been measured may have shifted by unknown amounts. In fact it is now recognized that *all* tide gauges are subject to slow rises and falls of land level, because the magma beneath the earth's crust is still slowly flowing back towards the regions occupied by thick ice sheets only about 10,000 years ago; however, outside tectonically active areas recent numerical models of this process appear to be successfully capturing the main features of this "postglacial rebound" (Peltier and Tushingham,1991).

Using these data, Gornitz and Lebedeff(1987) found that much of the variations from region to region could be removed if the tide gauge records were corrected for post glacial rebound. After correcting for this effect, Gornitz and Lebedeff found a global mean sea level rise of 1.2±0.3 mm/year. Two more recent estimates of global mean sea level rise in the

last century are 1.8±0.1 mm/year (Douglas, 1991) and 2.4±0.9 mm/year (Peltier and Tushingham, 1991). Both of the new estimates rely on a global model of postglacial rebound, which indicates that far away from the previously glaciated regions, coastal lands are rising relative to the sea. It is apparently the correction of this effect which leads to the discrepancy between Gornitz and Lebedeff's(1987) estimate and the two newer estimates. The sharpening of the estimate of sea level trends achieved by correcting for postglacial rebound is illustrated in Figure 20.5; note that the corrected trend is clearly greater than zero. However, Peltier and Tushingham(1991) report that their estimate of global mean sea level rise is "extremely sensitive to relatively modest alterations to the analysis procedure" which no doubt applies also to Douglas' estimate. All estimates are of necessity biased by the heavy concentration of available sea level records in Europe and North America.
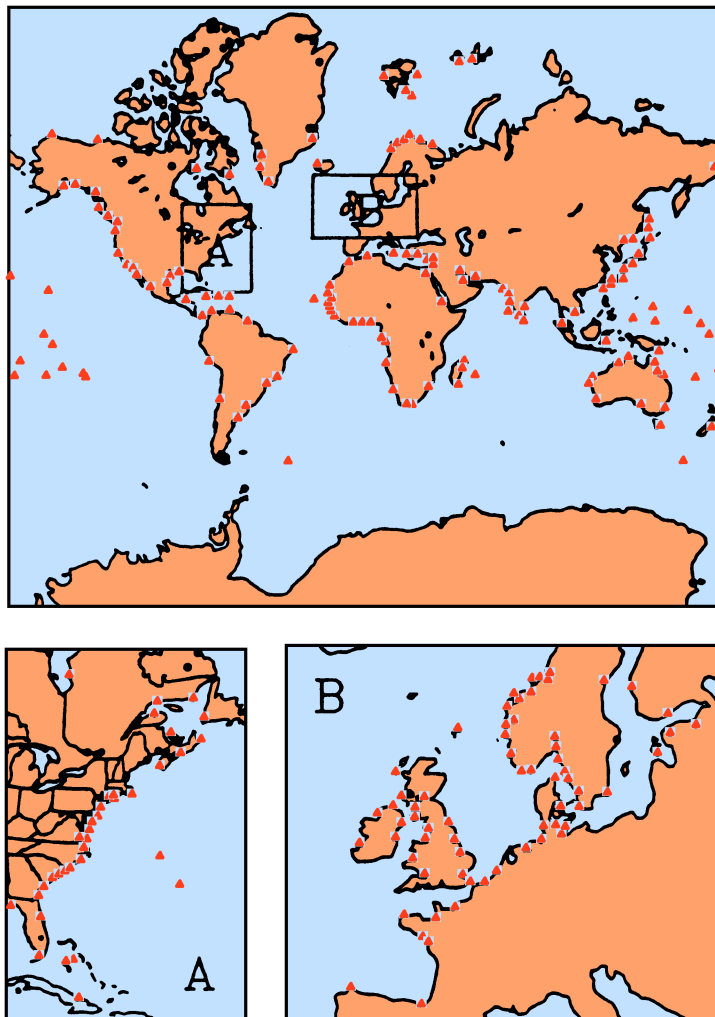

Fig. 20.4.

Locations of vali-dated tide gauges from which records are available that are of length greater than 10 years. The data are archived with the Permanent Service for Mean Sea Level at Bidston, Mersey-side, United King-dom.
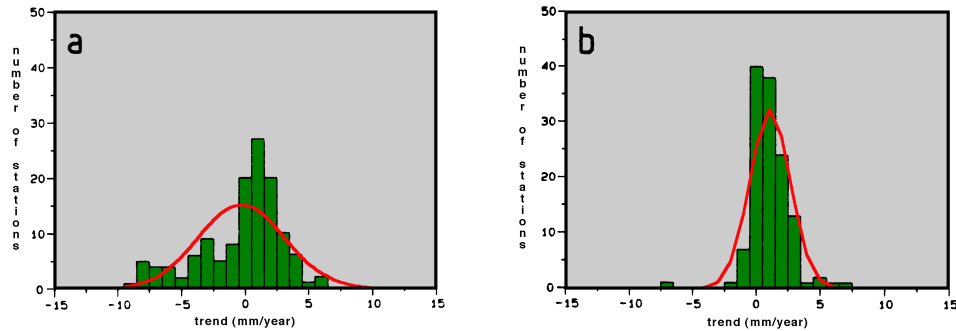
Adapted from Peltier and Tushingham (1991).

Fig. 20.5. Histograms of sea level trends from all tide gauge records with length of 50 years or longer, (a) before and (b) after correction for postglacial rebound. From Douglas (1991).

Much of this observed sea level rise can be accounted for by thermal expansion of seawater. As seen in Figure 20.1, the ocean has certainly warmed at the surface in the last century, and water expands upon warming. Convergence of Ekman transports and the convective overturn of water after surface cooling results in downward motions in certain parts of the ocean. Both processes provide the principal means by which warmed water is carried below the ocean surface; it is an advective rather than a diffusive process, so its magnitude can be directly estimated from large-scale ocean observations of currents. This makes it somewhat easier to assess thermal expansion rates for a given history of global mean surface temperature rise. The subducted water tends to accumulate in the subtropical gyres. However, Kelvin and Rossby waves tend to redistribute the warming over the rest of the globe; if this process went to completion, and the wind stress field did not change, the increase in depth-integrated steric height would be uniform over the world. This results in a rise in surface steric height (i.e. sea level) that is fairly spatially uniform, though thermal expansion rates are predicted to be somewhat greater in the tropics than near the poles (Figure 20.6). For the global mean SST rise of 0.4°-0.6°C per century inferred from Figure 20.1, the model yields a global mean thermal expansion of 0.8±0.2 mm/year.
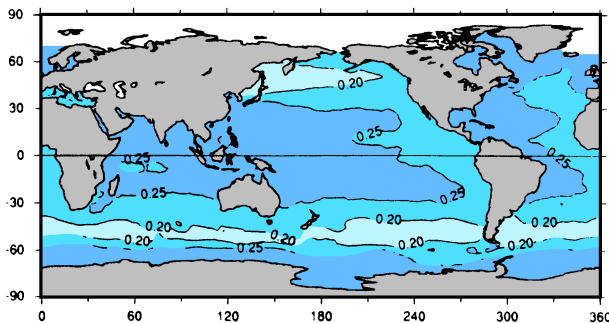

Fig. 20.6. Estimated sea level rise (m) by 2050 caused by thermal expansion, from the model of Church *et al.* (1991), assuming a global averaged temperature increase of 3°C by 2050.

A complete assessment of sea level rise has to include a number of other factors. The volume of water generated by the observed melting of non-polar glaciers over the last century is equivalent to a sea level rise of 0.46±0.26 mm/year (Meier, 1984). It is seen that the two effects together, thermal expansion and non-polar glacier melt, yield between them sea level rise estimates of 1.3±0.5 mm/year, somewhat below the most recent estimates quoted above (1.8±.1 mm/year; 2.4±.9 mm/year). The uncertainties in the remaining contributions are certainly large enough to account for the discrepancy. The effects of a warming on Greenland and Antarctica are believed to be of opposite sign, and neither is well known — the large ice sheets on Greenland's flanks are thought to have retreated under warmer conditions, whereas Antarctica (and inner Greenland) are so cold that the warming should have produced little or no melting over the last century. Instead, increased sea temperatures should have generated increased snowfall over Antarctica and inner Greenland. The net contribution from both polar ice sheets is believed to be near zero. However, this can evidently only be a very approximate figure, and the uncertainty of our estimate of the total sea level rise in the last century is substantially greater than the figure of ±0.5 mm/year from thermal expansion and non-polar ice melt alone.

Contributions of both signs arise also in consideration of groundwater, the water trapped on or under land masses. Artesian bores have removed substantial quantities of groundwater over the last century, while large water storages for hydroelectric dams etc. have been created. Newman and Fairbridge (1986) estimate that the latter effect would have reduced sea level by up to 0.75mm/year from 1957-1980, mostly in small water storages. The USSR Committee for the International Hydrologic Decade (Korzun, 1978) estimated a sea level rise of 0.8 mm/year due to reduction of groundwater storage.

In summary, our best estimate at present is that the combined contribution from groundwater and ice storage to sea level rise has been positive over the last century, and perhaps of the same order of magnitude as the combined contribution from thermal expansion and non-polar ice melt. However, in the absence of better information, the most recent projections of future sea level rise assume that there will be no net contribution from polar ice and groundwater.

Regional variations of sea level on decadal time scales

Before leaving the topic of long-term sea level change it is worth noting that after correction for postglacial rebound, other observations of interest from the point of view of decadal sea level change can be extracted from the available sea level records on the eastern coast of the USA and Canada.

Significant differences in the rate of sea level rise do occur from place to place, that probably originate in oceanographic effects. When sea level, corrected for postglacial rebound, from tide gauges along the North American east coast is examined for a trend over the period 1930-1980, it is found that over the 50-year interval sea level rose about 0.05 m more at gauges south of 38°N than at gauges to the north of 38°N (Figure 20.7). No tectonic explanation for this feature is known. The most likely cause is that the Gulf Stream altered its strength over the period. A very strong mean drop in steric sea level of order 0.7 m, about the strongest in the world ocean, is associated with the separation of the Gulf Stream from the coast near 35-38°N. The break in sea level trends over the past 50

years seen in Figure 20.7 occurs quite close to this mean sea level drop. It is rather reasonable to suppose that the 0.7 m sea level drop might have changed by 0.05 m, or 7%, over the last 50 years due to changes in climate.

Fig. 20.7. Trends of sea level (corrected for postglacial rebound) on the North American east coast, 1930-1980, plotted as a function of latitude. From Douglas (1991).
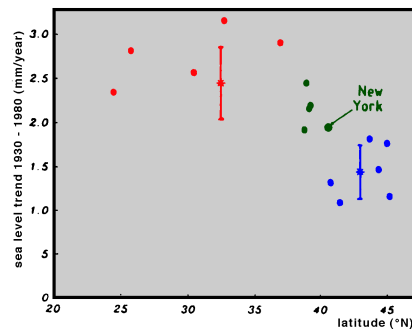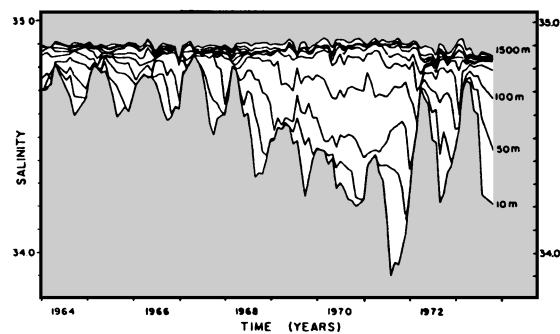
Fig. 20.8. Time series of monthly mean salinities at Ocean Weather Station Bravo, (56°30'N, 51°W), for 1964-1974. From Lazier (1980).

Ocean hydrology

The third source of long-term data for the ocean comes from accurate hydrological observations made by ocean research vessels and Ocean Weather Stations. The latter are vessels that have been stationed at fixed locations for some decades to supplement the land-based meteorological observation network and provide advance warning of weather events approaching the continents. Figure 20.8 shows a time series of monthly average salinity profiles based on data collected daily from Ocean Weather Station Bravo (56°30'N, 51°00'W) near the centre of the Labrador Sea. Freshening in late summer is evident at 10 m each year; in winter, salinity increases due to sea-ice formation. In most winters, a slight freshening can be seen at and below 100 m, bringing winter salinities close together over the top several hundred meters; this is due to convective overturn of the relatively fresh but cold waters above. Maximum mixed layer depths reached to over 1000 m in the winters of 1964-65, 1966-67, 1971-72 and 1972-73. However, from 1967-1971 the surface salinity was significantly lower than in other years, and mixed layers in these winters only penetrated to

200 m. Lazier (1980) suggested that abnormal northerly winds during these years blew sea ice southward, leading to greater ice melt in summer.

Brewer *et al*. (1983) complemented Lazier's work by examining two salinity sections across the Atlantic near 57°N, one taken in 1962 and the other in 1981. They found a systematic salinity decrease of about 0.02 between the two cruises. A plot of mean and standard deviation of salinity as a function of σ_{1000} from each cruise is seen in Figure 20.9 (σ_{1000} is the density the water would have if it was brought to 1000 m without changing salinity or potential temperature). The freshening is particularly evident when σ_{1000} is greater than 37.1 and for the range $36.8 < \sigma_{1000} < 36.9$. The first of these water mass modifications is thought to originate north of Denmark Strait, the latter in the Labrador Sea. These studies show that widespread changes in deep water can occur quite rapidly in response to rather modest changes in atmospheric conditions.
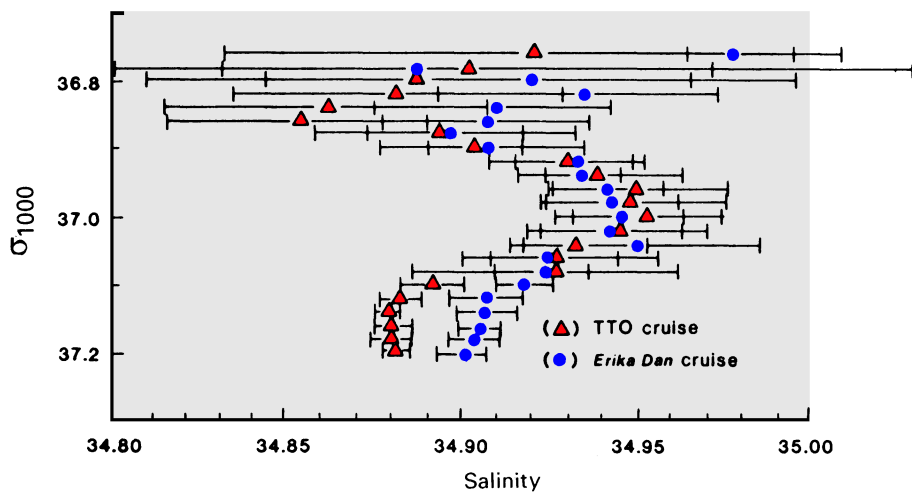

Fig. 20.9. Salinity means and standard deviations (horizontal bars) from two cruises across the North Atlantic near 57°N (dots for the 1962 cruise, triangles for the 1981 cruise) as functions of density σ_{1000} (for explanation see text). Note the clear freshening of the later curve, below $\sigma_{1000} = 37.1$ (corresponding to potential temperatures of about 2.5°C) and for σ_{1000} near 36.8 - 36.9. From Brewer *et al*. (1983) .

These deep water effects are not the only large-scale changes that have been observed in the north Atlantic Ocean over the last few decades. Levitus (1989) undertook a statistical study of the changes in the north Atlantic circulation from 1955-59 to 1970-74, using the data bank of all historical hydrographic observations. Unfortunately the north Atlantic Ocean is the only region where sufficient data exist to make such an analysis possible on a basin-wide scale. Figure 20.10b shows the difference in the depth of the 26.5 σ_θ surface for 1970-74 against 1955-59. Evidently, the thermocline shallowed significantly in most of the subtropical gyre, with some deepening on the inshore edge of the Gulf Stream. The net

appearance is of significant weakening of the density gradients across the Gulf Stream over this period, and hence (through geostrophy) a weakening of the near-surface Gulf Stream itself. However, a time series (Figure 20.10c) of the depth of the 26.5 σ_θ surface at 32°N, 64°W near the maximum depth of this isopycnal surface suggests that the shallowing near this location is not part of a longer-term trend but is associated with a minimum depth of the isopycnal surface in the early 1970s. Much more systematic monitoring of the oceans is required to link these observations with possible climate trends.

These broad-scale changes in the Atlantic subtropical gyre seem to involve changes in isopycnal depths without much clear signal in the water mass structure. Changes in water mass properties can be investigated by monitoring changes of potential temperature for given densities. As an example, Figure 20.11 shows the change in potential temperature on potential density surfaces along 49.5°W. A systematic cooling and therefore freshening is apparent north of 45°N; though it should be noted that this is a near-surface effect (water with $\sigma_\theta < 27.5$ is confined to the top 200 m at these latitudes).
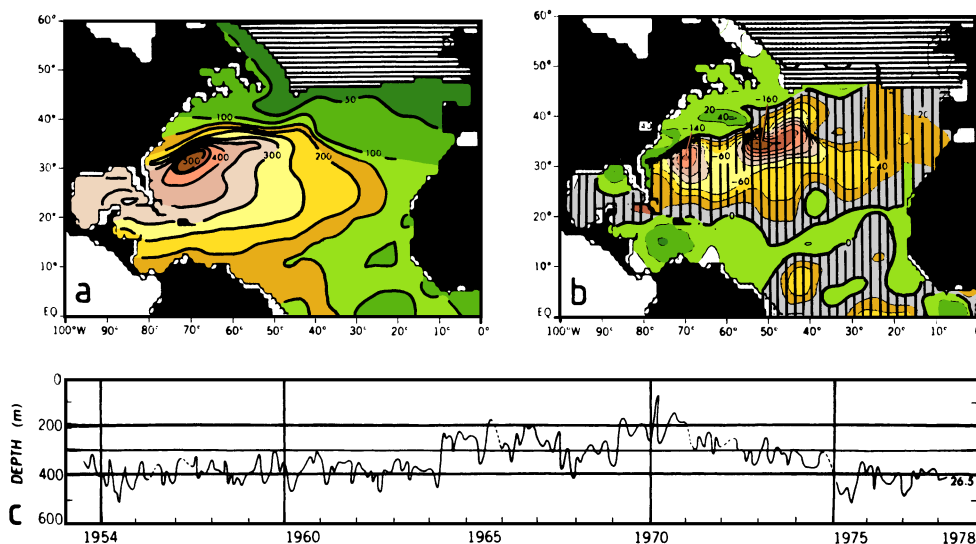

Fig. 20.10. Changes in thermocline depth in the North Atlantic Ocean. (a) Depth (m) of the 26.5 σ_θ surface for 1955-1959; hatching indicates regions where the surface does not exist, (b) depth difference (m) of the 26.5 σ_θ surface 1970-74 minus 1955-59, (c) depth of the 26.5 σ_θ surface at 32°N, 64°W for 1954-1978. Adapted from Levitus (1989).

It would be useful to extend such studies to the Southern Hemisphere, but opportunities for doing so are unfortunately rare. One recent example uses hydrographic sections at 43°S and 28°S in the western South Pacific Ocean taken in 1967 and repeated in 1989-90. Over the 22 years between these sections, there has been a depth-averaged warming at most depths below the surface mixed layer (Bindoff and Church, 1992). As in the case of the Atlantic Ocean, these changes are mostly due to changes in isopycnal depth with rather

little change in water mass properties on surfaces of constant density. A slight freshening for water of temperature 8°C or higher can account for a rise in sea level of about 2-3 cm, roughly equal to the observed rate of sea level rise over 20 years.

In conclusion, it will be evident from these examples that, while interdecadal variations definitely have occurred on basinwide scales in the ocean, our ability of keeping track of these interdecadal changes observationally is extremely sketchy. This needs to be borne in mind when considering results from numerical model studies.
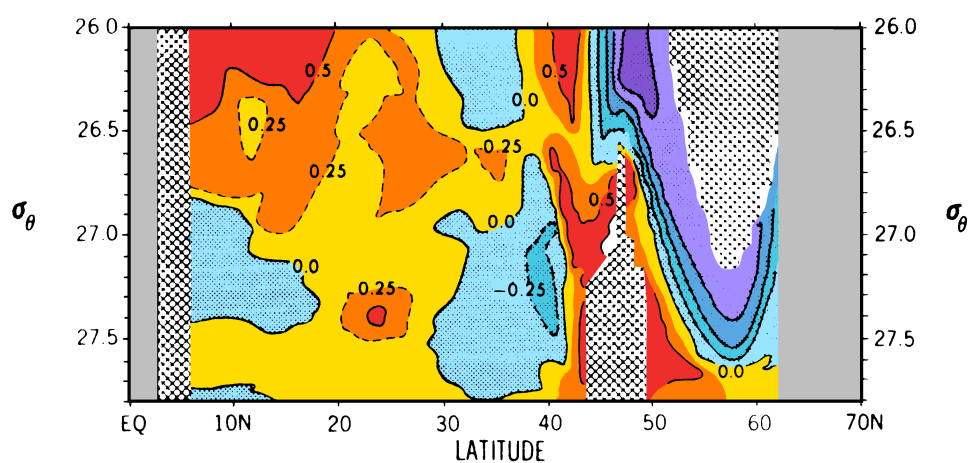

Fig. 20.11. Change of potential temperature 1970-1974 minus 1955-1959 (°C) on potential density surfaces along 49.5°W, as a function of potential density. Cross-hatching indicates regions where the corresponding potential density does not exist. From Levitus (1989).

Model results, salinity and climate

In an attempt to extend our understanding of long-term climate change beyond the limits posed by the available data, several research groups have begun the task of developing numerical models of the coupled ocean/atmosphere system. Such models require massive computing power, which is becoming available now. When applied to a simulation of our present climate, most models give satisfactory results when the ocean or the atmosphere are modelled in isolation but develop unreasonable climate trends (e.g. a rapid warming of the ocean surface) when the two components are treated as a coupled system. The salt budget proves to be particularly difficult, most probably because we do not yet understand how to incorporate the process of tropical rainfall correctly. A number of more or less empirical methods have been developed to prevent the models from diverging from the known climate trend of the last decades. Our hope is that by applying these methods to simulations into the future we can get reasonably accurate estimates of future climate trends.

One of the most intriguing results from these models is the role of sea surface salinity. Models which simulate the oceanic and atmospheric circulation for several thousand years

have revealed the existence of (at least) two stable steady states. One of these steady states corresponds to the circulation system we observe today, with North Atlantic Deep Water formation and recirculation through all ocean basins. The other steady state does not have North Atlantic Deep Water formation; it shows a very much colder and fresher north Atlantic Ocean and very little Deep Water exchange between the three major oceans. Figure 20.12 shows the SST difference between the two possible steady solutions. Compared to the present situation, the solution without NADW formation shows the north Atlantic Ocean colder by as much as 7°C and the north Pacific Ocean colder by some 2°C. The qualitative resemblance between Figure 20.12 and the third EOF derived from SST data (Figure 20.3a) is striking; however the amplitude of the SST differences of Figure 20.12 is larger than the largest differences associated with the third EOF by a factor of 5. One way of interpreting this is to say that the data support the possibility of an alternative steady state of the oceanic circulation, in the sense that the time function $G_3(t)$ can be seen as an indicator for the speed with which the ocean circulation may be changing from one steady state to the other.
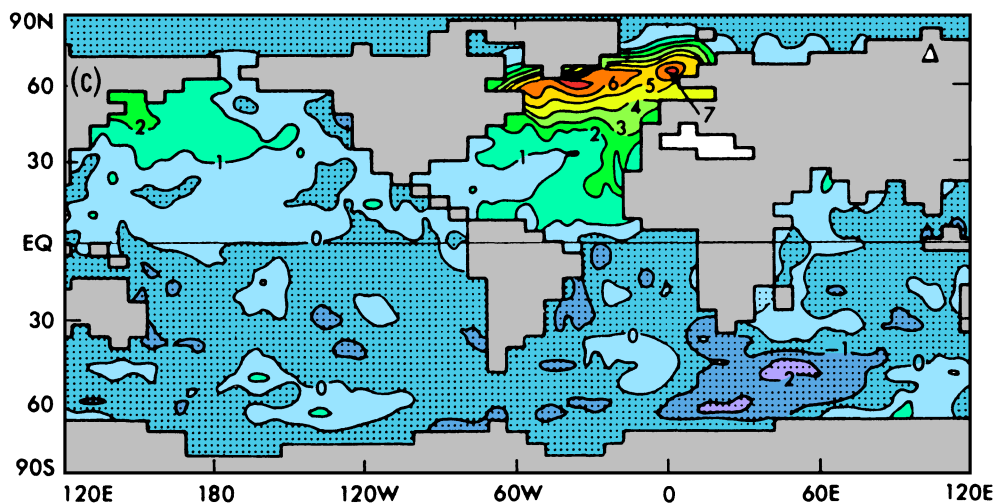

Fig. 20.12. Difference in sea surface temperature, $T_1 - T_2$ (°C), between two stable steady states of the oceanic circulation found in a coupled ocean/atmosphere model. T_1 is SST in the model with NADW formation, T_2 is SST in the model without NADW formation. From Manabe and Stouffer (1988).

The existence of two steady states may seem to contradict our argument from Chapter 18 that a cold but fresh north Atlantic Ocean will eventually return to its present state by increasing its salinity through water vapour export across Central America. However, if the change in north Atlantic SST is large enough (and a 7°C SST difference is an enormous change) it might be expected to have a major effect on the atmospheric circulation and associated rainfall which might result in a suppression of water vapour export from the Atlantic Ocean. A large shift in the distribution of tropical rainfall was indeed found in the

coupled model; however, as already mentioned, modelling tropical rainfall is one of the weak points of all models at present.

   Whether the ocean circulation (within the confines of the present world topography) can, or did in the past, have more than one stable steady state as indicated by models, is a subject for paleoceanography. Whatever the answer will be, there is no doubt that the north Atlantic Ocean is the major determinant of the process. Consider the sketch shown in Figure 20.13. Deep convection in the Greenland Sea will be inhibited if the salinity in the northward flow of water from the subtropics is reduced; this is the mechanism behind Figure 20.12. The same effect would be observed if the amount of freshwater and ice exported from the Arctic Ocean is increased to cover the surface layer of the Greenland and Iceland Seas. This would force the warm, salty water from the south to submerge below the fresher surface water well before entering the Greenland Sea (in today's climate it does not submerge until it reaches the Greenland Sea; see Chapter 7). The fresh surface layer would insulate the underlying subtropical water and prevent it from cooling, stopping the deep convection in the Greenland Sea. Formation of North Atlantic Deep Water can thus be inhibited by various means, and it seems more and more likely that circulation patterns without NADW formation did exist in the past. To give just one example, sediment cores from the Antarctic Circumpolar Current region show large variations in carbon isotope composition between periods of glaciation and interglacial periods, which can be related to changes in the NADW contribution to Circumpolar Water (Charles and Fairbanks, 1992) and suggest that NADW formation was much reduced during the last ice age. This of course means that a circulation with very little or no NADW formation can develop again. Does the introduction of greenhouse gases into the atmosphere promote the change to such a pattern, or does it stabilize the existing circulation? The answer, although impossible to give today, is of tremendous interest to the people of Europe, which would see drastic changes if the north Atlantic sea surface temperature were to fall by several °C.
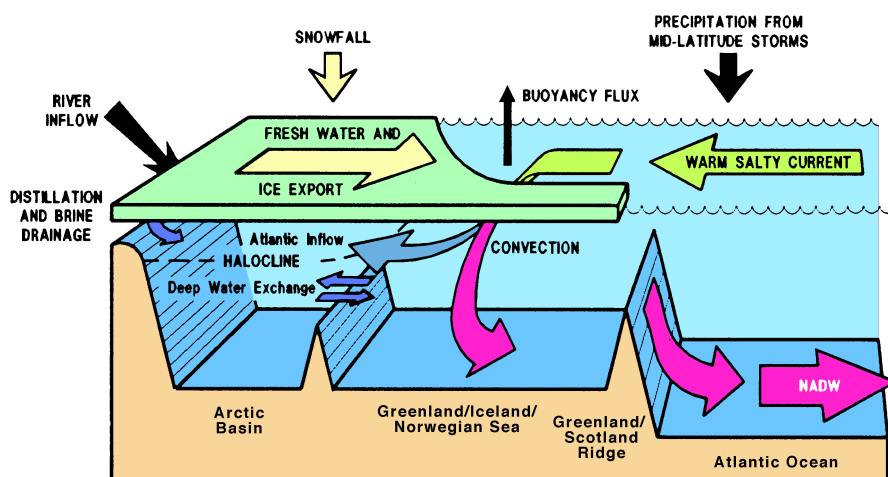

Fig. 20.13. Sketch of the circulation in the north Atlantic Ocean.

While the model results and possible scenarios are extremely interesting, they are only indicative of the types of phenomena that may occur in the real coupled ocean-atmosphere system. They give us no indication, for example, whether the fluctuations of the north Atlantic gyre discussed above are associated with some coupled ocean-atmosphere fluctuation or merely a response to random fluctuations in atmospheric forcing; nor do we have the data to know if such phenomena are occurring in most of the other basins. Regional oceanographers and modellers agree that there is a lamentable gap between the comprehensive global coverage of the ocean apparently provided by models and the extraordinarily sparse nature of the data base with which to verify them. We will certainly be living with this problem for some decades. However, oceanographers are devoting considerable efforts to improving the situation. The World Ocean Circulation Experiment (WOCE) introduced in Chapter 2 is one component of the strategy, TOGA (see Chapter 19) another. Out of these efforts will evolve the Global Ocean Observation System (GOOS) as the equivalent of the network of meteorological observations supported by all member countries of the World Meteorological Organization (WMO). Although it will have a very similar function, namely the provision of real-time data for the forecasting of the oceanic circulation, it will have to be based on very different technology. Factors affecting its design are the lack of availability of voluntary observers for many ocean regions and the - in comparison to atmospheric space scales - much smaller scales of oceanic eddies and frontal variability. The increased demand posed by small space scales is partly compensated by the much longer oceanic time scales which allow less frequent sampling than in the atmosphere. Scientists involved in the design of GOOS are actively working on questions of data resolution in space and time required for forecasting the variability of the oceanic circulation.